5-1-2017

Skeletal Muscle PGC-1β Signaling is Sufficient to Drive an Endurance Exercise Phenotype and to Counteract Components of Detraining in Mice

Samuel Lee
Sanford Burnham Prebys Medical Discovery Institute

Teresa C. Leone
Sanford Burnham Prebys Medical Discovery Institute

Lisa Rogosa
Sanford Burnham Prebys Medical Discovery Institute

John Rumsey
Sanford Burnham Prebys Medical Discovery Institute

Julio Ayala
Sanford Burnham Prebys Medical Discovery Institute

See next page for additional authors

Accepted version. *American Journal of Physiology: Endocrinology and Metabolism,* Vol. 312, No. 5 (May 2017): E394-E406. DOI.

American Journal of Physiology : Endocrinology and Metabolism, Vol. 312, No. 5 (May 2017): E394-E406. DOI.

Skeletal Muscle PGC-1β Signaling Is Sufficient to Drive An Endurance Exercise Phenotype And To Counteract Components Of Detraining In Mice

Samuel Lee
Center for Metabolic Origins of Disease, Sanford Burnham Prebys Medical Discovery Institute, Orlando, Florida
Teresa C. Leone
Center for Metabolic Origins of Disease, Sanford Burnham Prebys Medical Discovery Institute, Orlando, Florida
Lisa Rogosa
Center for Metabolic Origins of Disease, Sanford Burnham Prebys Medical Discovery Institute, Orlando, Florida
John Rumsey

Center for Metabolic Origins of Disease, Sanford Burnham Prebys Medical Discovery Institute, Orlando, Florida

Julio Ayala

Center for Metabolic Origins of Disease, Sanford Burnham Prebys Medical Discovery Institute, Orlando, Florida

Paul M. Coen

Center for Metabolic Origins of Disease, Sanford Burnham Prebys Medical Discovery Institute, Orlando, Florida

Translational Research Institute for Metabolism and Diabetes, Florida Hospital, Orlando, Florida

Robert H. Fitts

Department of Biological Sciences, Marquette University, Milwaukee, Wisconsin

Rick B. Vega

Center for Metabolic Origins of Disease, Sanford Burnham Prebys Medical Discovery Institute, Orlando, Florida

Daniel P. Kelly

Center for Metabolic Origins of Disease, Sanford Burnham Prebys Medical Discovery Institute, Orlando, Florida

Abstract

Peroxisome proliferator-activated receptor-γ coactivator (PGC)-1α and -1β serve as master transcriptional regulators of muscle mitochondrial functional capacity and are capable of enhancing muscle endurance when overexpressed in mice. We sought to determine whether muscle-specific transgenic overexpression of PGC-1β affects the detraining response following endurance training. First, we established and validated a mouse exercise-training-detraining protocol. Second, using multiple physiological and gene expression end points, we found that PGC-1β overexpression in skeletal muscle of sedentary mice fully recapitulated the training response. Lastly, PGC-1β overexpression during the detraining period resulted in partial prevention of the detraining response. Specifically, an increase in the plateau at which O_2 uptake ($\dot{V}o_2$) did not change from baseline with increasing treadmill speed [peak $\dot{V}o_2$ ($\Delta\dot{V}o_{2max}$)] was maintained in trained mice with PGC-1β overexpression in muscle 6 wk after cessation of training. However, other detraining responses, including changes in running performance and in situ half relaxation time (a measure of contractility), were not affected by PGC-1β overexpression. We conclude that while activation of muscle PGC-1β is sufficient to drive the complete endurance phenotype in sedentary mice, it only partially prevents the detraining response following exercise training, suggesting that the process of endurance detraining involves mechanisms beyond the reversal of muscle autonomous mechanisms involved in endurance fitness. In addition, the protocol described here should be useful for assessing early-stage proof-of-concept interventions in preclinical models of muscle disuse atrophy.

Skeletal muscle endurance and resistance to fatigue are determined by a variety of factors, including the capacity to store and oxidize high-energy fuels, cardiovascular capacity, and the proportion of oxidative slow-twitch, insulin-sensitive fibers needed for persistent mechanical function. Muscle detraining occurs with periods of reduced ambulation or complete immobilization, such as during

recuperation from acute injuries or illness. The detraining response is manifest as reduced muscle performance associated with a diminution of mitochondrial functional capacity, reduced blood vessel density, reduction in the proportion of oxidative muscle fibers, and relative insulin resistance (1, 5, 29, 40). The detrained state increases injury recovery time and enhances the risk of subsequent injury or concurrent illness/infection (12). In addition, sarcopenia may synergize with untrained or detrained states, often leading to "failure-to-thrive" syndrome in the elderly, a condition with significant morbidity and mortality rates (8). Detraining effects are prevalent in highly trained individuals, and the magnitude of the detraining response is dramatic in this highly fit population. Moreover, athletes and other highly trained individuals, such as infantry soldiers, could be susceptible to reinjury or new injuries, such as muscle tears, tendonitis, and even skeletal fractures, when remobilizing from the detrained state (20, 28).

Delineation of the molecular and cellular events involved in the muscle-detraining response requires insight into the training process. Endurance training triggers a variety of adaptive responses in muscle, including marked increases in mitochondrial content, vascularity, and proportion of oxidative muscle fibers, all of which are rapidly reversed following cessation of training (42, 54). Whole body insulin sensitivity and insulin-stimulated glucose transport are also significantly positively correlated with the trained state, related, at least in part, to the increase in proportion of oxidative fibers, which are highly insulin-responsive (13, 24, 34, 41, 48). The increase in muscle mitochondrial content with endurance training increases capacity for oxidation of fatty acids and glucose for ATP production (23, 25). Training also increases capacity for delivery of O_2 and nutrients through effects on cardiac output and by triggering an angiogenic response. Conversely, the detraining response results in a rapid reversal of these adaptive training responses in muscle, including oxidative fibers, mitochondrial content, vascularity, and, thus, capacity for muscle fuel oxidation (46, 54). The muscle-detraining response begins within 7 days after cessation of training (11, 26, 37). An important question relates to whether muscle detraining represents a simple reversal of the training process or also involves independent mechanisms. The answer to this key question has implications for the development of therapeutic strategies to prevent muscle detraining during periods of immobilization.

Significant advances have been made in identifying critical upstream regulators of the muscle endurance-training response. Specifically, the muscle-enriched transcriptional coactivators peroxisome proliferator-activated receptor-γ (PPARγ) coactivator (PGC)-1α and -1β have been shown to activate features of endurance training in skeletal muscle in transgenic mice (3, 4, 22, 32, 33, 35). The PGC-1 isoforms are known to be necessary for development of high-capacity mitochondrial systems in heart and skeletal muscle (15, 30, 38). PGC-1α gene expression is induced in skeletal muscle in physiological conditions that demand increased energy expenditure, such as short- and long-term exercise in animal models and in humans (7, 15, 21, 31, 43, 52). Tissue-specific transgenic approaches in mice have shown that forced overexpression of PGC-1 coactivators in skeletal muscle increases muscle oxidative capacity and the proportions of oxidative fibers (35). Notably, transgenic strategies have shown that PGC-1β coordinately drives formation of muscle oxidative fibers (4) and stimulates angiogenesis (44) in mice. Mouse PGC-1α and -1β transgenic and gene deletion studies have also demonstrated the important role of these factors in maintaining mitochondrial function (53) and defending against inflammation (14) and oxidative damage (17).

The objectives of this study were severalfold. *1*) It was necessary to establish a protocol that allows in-depth analysis of the physiological, cellular, and molecular responses to muscle detraining in mice. *2*) We sought to further explore the role of PGC-1β in the muscle endurance phenotype. We chose to focus on PGC-1β, given that this transcriptional coregulator has been shown to trigger multiple components of the endurance fitness response, including energy metabolism, angiogenesis, and fiber type shifts (4, 44). In addition, less is known about the role of PGC-1β than PGC-1α in regulating physiological responses. *3*) We sought to determine whether maintenance of the PGC-1β-induced trained state impacts the muscle-detraining response following cessation of an endurance-training regimen. To accomplish these goals, we employed a conditional mouse transgenic line that allows muscle-specific induction of PGC-1β. We found that forced expression of PGC-1β in muscle was sufficient to fully activate the endurance-training response in sedentary mice. However, only a subset of the detraining responses was prevented by PGC-1β overexpression during the period of detraining following cessation of exercise, suggesting that other mechanisms, possibly including factors external to muscle, are at play. The protocol described here should be useful for preclinical assessment of the impact of various interventions on specific components of the muscle-detraining response.

METHODS

Transgenic mice.

Animal studies were conducted in strict accordance with National Institutes of Health guidelines for humane treatment of animals. Transgenic mice expressing a muscle-specific tetracycline-regulatable transactivator (tTA) driven by the muscle creatine kinase promoter (MCK-tTA) are described elsewhere (19). To create the PGC-1β transgene, mouse PGC-1β cDNA with an NH_2-terminal flag tag was inserted into the pTRE2 vector (Clontech). This construct was linearized with *Aat*II and *Ase*I and injected into fertilized mouse eggs to generate the tetracycline response element (TRE)-PGC-1β lines. Mice carrying the transgene were identified by a transgene-specific PCR assay. These two strains, both in the FVB/N genetic background, were crossed to generate double-transgenic [Tet-off PGC-1β, or TRE-PGC-1β(+)] mice. Breeding pairs and offspring were maintained on chow containing doxycycline (200 mg/kg; Research Diet, Brunswick, NJ). To activate the TRE-PGC-1β transgene, doxycycline-containing chow was removed and replaced with standard chow (diet 2916, Teklad), which removes suppression from the TRE that drives expression of PGC-1β. All animal experiments and euthanasia protocols were conducted in accordance with National Institutes of Health guidelines for humane treatment of laboratory animals and were reviewed and approved by the Animal Care Committee of Sanford Burnham Prebys Medical Discovery Institute at Lake Nona.

Experimental design.

To determine whether PGC-1β attenuates the effects of detraining, the following experimental design was employed (Fig. 1). From birth, mice were maintained on doxycycline-containing chow to inactivate the TRE (51). At 8 wk of age, body composition of male FVB/N TRE-PGC-1β(−) and TRE-PGC-1β(+) mice (each with 1 copy of the MCK-rtTA allele) was determined by NMR (MiniSpec, Brucker, The Woodlands, TX), and maximal O_2uptake ($\dot{V}o_{2max}$) studies were performed. Mice were divided into two groups: Sedentary and Runner. The Runner mice were singly housed with a Kay-tee Run-Around Mini Exercise running wheel (4.5 inch) for 8 wk. The Sedentary mice were housed according to normal procedure. At 2 wk before the wheel was removed from the cage, doxycycline-containing chow was replaced with

standard chow (Teklad Diet 2916) to induce PGC-1β expression in the TRE-PGC-1β(+) mice (Fig. 1). At 2, 4, 6, and 8 wk following doxycycline removal, NMR and $\dot{V}o_{2max}$ studies were repeated. Tissue was harvested for gene expression analysis 2 days after the final $\dot{V}o_{2max}$ study.

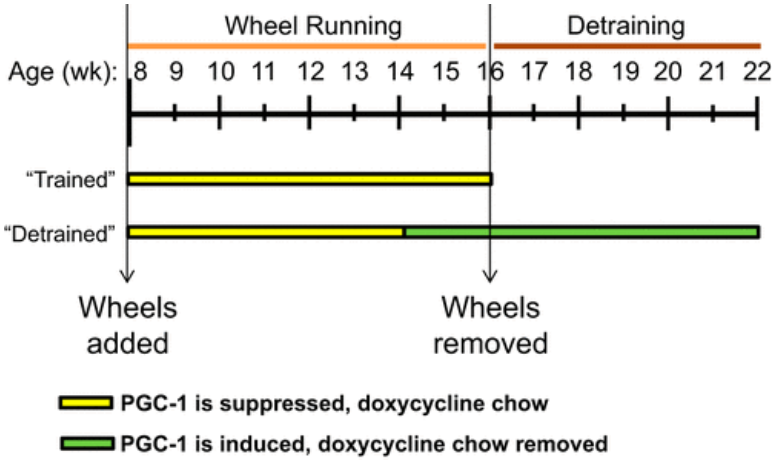

Fig. 1. Longitudinal study timeline. Mice were segregated into Sedentary and Runner groups and harvested 8 wk after training (Trained) or 6 wk after detraining (Detrained). Running wheels were added to cages of Runner mice (singly housed) at 8 wk of age. All cages were maintained on doxycycline-containing chow to suppress induction of peroxisome proliferator-activated receptor-γ coactivator (PGC)-1β. Doxycycline was removed 2 wk before the start of detraining to induce expression of PGC-1β before removal of the running wheels, which occurred 8 wk after the wheels were added to the cages.

Mitochondrial respiration studies.

Complex II-supported mitochondrial respiration was assessed in saponin-skinned permeabilized soleus fibers with succinate as substrate and in the presence of rotenone, as previously described (33, 45). Briefly, 8- to 16-wk-old male Sedentary and Runner mice were anesthetized, and soleus fibers were separated and transferred to a buffer [in mM: 2.77 K_2Ca-EGTA, 7.23 K_2EGTA, 6.56 $MgCl_2$, 20 imidazole, 53.3 K-MES, 20 taurine, 5.3 ATP, 15 PCr, 3 KH_2PO_4, and 0.5 DTT (pH 7.1)] supplemented with 50 µg/ml saponin and permeabilized for 30 min at 4°C with gentle stirring. Fibers were then washed twice for 10 min each in buffer containing 2.77 mM K_2Ca-EGTA, 7.23 mM K_2EGTA, 1.38 mM $MgCl_2$, 20 mM imidazole, 100 mM K-MES, 20 mM taurine, 3 mM KH_2PO_4, 0.5 mM DTT, and 2 mg/ml BSA (pH 7.1). Respiration was measured at 37°C using an optical probe (Oxygen FOXY Probe, Ocean Optics, Dunedin, FL). After measurement of basal state 2 respiration, ADP-stimulated state 3 respiration was determined by exposure of fibers to 1 mM ADP. State 4 respiration was evaluated following addition of oligomycin (1 µg/ml). Solubility of O_2 in the respiration buffer at 25°C was taken as 246.87 nmol O_2/ml. Respiration rates were expressed as nmol $O_2 \cdot min^{-1} \cdot$mg dry wt^{-1}.

Exercise studies and $\dot{V}o_{2max}$ testing.

Mice were acclimated (run for 9 min at 10 m/min followed by 1 min at 20 m/min) to the treadmill for 2 consecutive days before the experimental protocol.

For the low-intensity distance-to-exhaustion protocol, fed mice were run on a 5% slope for 10 min at 10 m/min followed by an increase of 2 m/min for 15 min and every 15 min thereafter, not exceeding

36 m/min, until exhaustion (5 consecutive seconds on the shock grid). The high-intensity distance-to-exhaustion protocol was performed in conjunction with the $\dot{V}o_{2max}$ studies described below.

The plateau at which change from the average baseline $\dot{V}o_2$ ($\Delta\dot{V}o_2$) did not change with increasing treadmill speed [peak $\dot{V}o_2$ ($\Delta\dot{V}o_{2max}$)] and respiratory exchange ratio (RER) were determined as described previously (6, 9). Briefly, 2- to 6-mo-old male mice were placed in an enclosed treadmill attached to the Comprehensive Laboratory Animal Monitoring System (CLAMS, Columbus Instruments) and allowed to acclimate for 30 min at a 0° incline and 0 m/min. A baseline $\dot{V}o_2$ was calculated as the average of $\dot{V}o_2$ values during the last 5 min of the acclimation period. The mice were then challenged with intervals of increasing speed (4 m/min every 3 min). A shock grid was used to encourage the mice to run. $\dot{V}o_2$ was measured every minute before the exercise challenge, throughout the challenge, and following exhaustion. High-intensity distance to exhaustion was calculated from the same study.

Histological analyses and electron microscopy.

Mouse gastrocnemius was collected, immersed in gum tragacanth-phenol, and frozen on an embedding block (catalog no. 6755810, Fisher Scientific) with isopentane that had been cooled in liquid nitrogen. CD31 staining was visualized using chromogenic 3,3′-diaminobenzidine. Samples on frozen slides were fixed in 10% neutral buffered formalin for 15 min, washed in water, and placed on the Discovery XT instrument (Ventana Medical Instruments). CD31 antibody (catalog no. DIA-310 clone SZ31, Dianova) was used at a 1:25 dilution for 1 h. Muscles for myosin heavy chain (MHC) immunofluorescence analysis were embedded as noted above, and immunofluorescence was performed as described previously (50). The fibers were stained using antibodies from the Developmental Studies Hybridoma Bank: MHC1, yellow (antibody BA-F8); MHC2a, red (antibody SC-71); MHC2x, black (unstained); and MHC2b, green (antibody BF-F3). After the slides were stained, they were scanned on the Aperio ScanScope XT.

Electron microscopy was performed on soleus muscle rapidly fixed with Karnovsky's fixative (2% glutaraldehyde, 1% paraformaldehyde, and 0.08% sodium cacodylate), as previously described (53). Sectioning was performed by the Histology Core Facility at Sanford Burnham Prebys Medical Discovery Institute at Lake Nona, and the images were visualized on a Philips FEI Morgagni transmission electron microscope (Sanford Burnham Prebys Imaging Core Facility).

RNA and genomic DNA analyses.

Total RNA was isolated from mouse skeletal muscle using the RNAzol method (Tel-Test, Friendswood, TX). Real-time quantitative RT-PCR was performed using the Stratagene MX3005P detection system, and reagents were supplied by Stratagene. Arbitrary units of target mRNA were corrected to expression of ribosomal protein lateral stalk subunit P0 (*Rplp0*, 36B4). Specific oligonucleotide primers for target gene sequences are as follows: 5′-CAAGCAGCAACATGGGAAGA-3′ (forward) and 5′-GTCAGGATCAAGAACCGAAGTCT-3′ (reverse) for citrate synthase (*Cs*), 5′-GTCTGTCTTCGAGTCCGAACG-3′ (forward) and 5′-GGAGATTTGGTCCAGTCTTATGC-3′ (reverse) for cytochrome *c* (*Cycs*), 5′-CGTGAGGGCAATGATTTATACCAT-3′ (forward) and 5′-TCCTGGTCTCTGAAGTATTCAGCAA-3′ (reverse) for ATP synthase-β (*Atp5b*), 5′-TGCCTACGAGGTGATCAAGCT-3′ (forward) and 5′-GCACCCGCCTAAGGTTCTTC-3′ (reverse) for lactate dehydrogenase A (*Ldha*), 5′-AGTCTCCCGTGCATCCTCAA-3′ (forward) and 5′-AGGGTGTCCGCACTCTTCCT-3′ (reverse) for lactate

dehydrogenase B (*Ldhb*), 5′-CCCATGGCATTAGCCTCTTT-3′ (forward) and 5′-GCTGTGTCCTGAGCTTTCAT-3′ (reverse) for long-chain acyl-CoA dehydrogenase (*Acadl*), 5′-AGGCTTGGAAAAATCTGTCTC-3′ (forward) and 5′-TGCTCTTCCCAAGACTTCATT-3′ (reverse) for mitochondrial transcription factor A (*Tfam*), 5′-TCCAGAAGTCAGCGGCCTTGTGTCA-3′ (forward) and 5′-CTCTGGGACAGGGCAGCACCGA-3′ (reverse) for PGC-1β (*Ppargc1b*), 5′-CTCGGCGCTGACTCCG-3′ (forward) and 5′-CACACAGCTGTTCCTCTCCAG-3′ (reverse) for *Ppargc1b* (endogenous only), 5′-AGCAAGAAGAGCATCTGTGGG-3′ (forward) and 5′-ACCCTGCGTGTCAGAGAGATA-3′ (reverse) for *Ppargc1b* (trangene only), 5′-CGGAAATCATATCCAACCAG-3′ (forward) and 5′-TGAGAACCGCTAGCAAGTTTG-3′ (reverse) for PGC-1α (*Ppargc1a*), 5′-ACCAGAACACACGCTTCCTT-3′ (forward) and 5′-CCCATCACAGCCCATCTG-3′ (reverse) for PPAR-δ (*Ppard*), 5′-AGGAGTACGTCCTGCTG-3′ (forward) and 5′-CCTCAGCATCTTCAATG-3′ (reverse) for estrogen-related receptor (EsRR)-α (*Esrra*), 5′-ACGGCTGGATTCGGAGAAC-3′ (forward) and 5′-TCCTGCTCAACCCCTAGTAGATTC-3′ (reverse) for EsRR-β (*Esrrb*), 5′-TGACTTGGCTGACCGAG-3′ (forward) and 5′-CCGAGGATCAGAATCTCC-3′ (reverse) for EsRR-γ (*Esrrg*), 5′-GGCAGCAGCAGCTGCGGAAGCAGAGTCTGG-3′ (forward) and 5′-GAGTGCTCCTCAGATTGGTCATTAGC-3′ (reverse) for MHC2x (*Myh1*), 5′-GCCAACTATGCTGGAGCTGATGCCC-3′ (forward) and 5′-GGTGCGTGGAGCGCAAGTTTGTCATAAG-3′ (reverse) for MHC1 (*Myh7*), 5′-GGCACAAACTGCTGAAGCAGAGGC-3′ (forward) and 5′-GGTGCTCCTGAGGTTGGTCATCAGC-3′ (reverse) for MHC2a (*Myh2*), 5′-GAGCTACTGGATGCCAGTGAGCGC-3′ (forward) and 5′-CTGGACGATGTCTTCCATCTCTCC-3′ (reverse) for MHC2b (*Myh4*), 5′-CTGCAGGCATCGGCAAA-3′ (forward) and 5′-GCATTTCGCACACCTGGAT-3′ (reverse) for platelet and endothelial cell adhesion molecule 1 (*Pecam-1*, CD31), and 5′-TGGAAGTCCAACTACTTCCTCAA-3′ (forward) and 5′-ATCTGCTGCATCTGCTTGGAG-3′ (reverse) for *Rplp0* (36B4).

Genomic/mitochondrial DNA (mtDNA) was isolated using the RNAzol method followed by backextraction with 4 M guanidine thiocyanate, 50 mM sodium citrate, and 1 M Tris and an alcohol precipitation. The mtDNA content was determined by SYBR Green analysis (Stratagene). The levels of NADH dehydrogenase subunit 1 (*Nd1*, mtDNA) were normalized to the levels of lipoprotein lipase (*Lpl*, genomic DNA). The primer sequences are as follows: 5′-CCCATTCGCGTTATTCTT-3′ (forward) and 5′-AAGTTGATCGTAACGGAAGC-3′ (reverse) for *Nd1* and 5′-GGATGGACGGTAAGAGTGATTC-3′ (forward) and 5′-ATCCAAGGGTAGCAGACAGGT-3′ (reverse) for *Lpl*.

Antibodies and Western immunoblot studies.

Antibody directed against PGC-1β was generously provided by Anastasia Kralli (Scripps).

Western immunoblot studies were performed with whole gastrocnemius muscle lysates. Briefly, after gastrocnemius muscle was sonicated in RIPA buffer [1% NP40, 0.5% SDS, 100 mM phenylmethylsulfonyl fluoride, and cOmplete protease inhibitors (Roche)] on ice using a Branson Sonifier 450 with 50% duty cycle, insoluble cellular debris was removed by centrifugation (15,000 *g*). Protein was quantified using the Pierce Protein Determination Kit (bicinchoninic acid method). Lysate was run on a 7.5% SDS-polyacrylamide gel and transferred to a nitrocellulose membrane. The membranes were blocked with 5% nonfat dry milk for 1 h at room temperature and then probed with primary antibody for PGC-1β diluted 1:10,000 in 1% BSA with 0.1% Tween 20. The membranes were washed three times for 10 min each in 0.1% Tween in Tris-buffered saline and then probed with goat

anti-rabbit IRDye 800CW (1:8,000 dilution; catalog no. 827:08365, LI-COR)-labeled secondary antiserum in 0.1% Tween-5% nonfat dry milk blocking buffer for 1 h at room temperature. The membranes were imaged using a LI-COR Odyssey scanner. Detection and quantification were performed using Odyssey Image Studio software.

In situ muscle stimulation.

In situ tetanus force and low-frequency fatigue experiments were performed in mouse slow-twitch soleus and fast-twitch plantaris muscles. Before stimulation of the motor nerve, the animals were anesthetized by pentobarbital sodium (Nembutal) injection (100 mg/kg body wt ip). The muscles were isolated, with care taken to leave the blood and nerve supply intact, and stimulated as described previously (27) using the 1300A Whole Mouse Test System (Aurora Scientific, Aurora, ON, Canada). Core temperature was held at 37°C. The sciatic nerve was drawn into a suction electrode, and biphasic pulses were administered to elicit peak tetanic tension at 160 Hz for 200 ms (for plantaris) and 150 Hz for 300 ms (for soleus). Optimal muscle length was established, and peak tetanic force and half relaxation time were measured. Muscle fatigue testing was carried out for 20 min at 150 Hz with 200-ms trains (for soleus) and at 160 Hz with 100-ms trains (for plantaris) produced every second. After a 3-min rest period, a postfatigue tetanus was recorded; then the fatigued muscles were surgically removed and weighed.

Statistical analyses.

Data were analyzed by Student's *t*-test (2-tailed). Values are means ± SE. Statistical significance was defined as $P < 0.05$.

RESULTS

Validation of an endurance-detraining protocol for mice.

We first sought to develop and validate an endurance-detraining protocol for mice. Eight-week-old male wild-type FVB/N mice were trained for 8 wk on a voluntary running wheel. Mice that averaged <5 km/night were removed from the study. The remaining (Runner) mice ran, on average, 13–14 km/night. After this training regimen, a battery of endurance-training end points were used to compare the trained group with age- and strain-matched sedentary control mice. The Runner mice demonstrated a modest, but significant, reduction in body weight after the training period that was largely accounted for by a reduction in percent body fat (Fig. 2). Runner mice performed better on both low- and high-intensity run-to-exhaustion treadmill protocols (Fig. 3*A*). Mean $\Delta\dot{V}o_{2max}$ was significantly higher in the Runner mice posttraining (Fig. 3*B*). Notably, mean $\Delta\dot{V}o_{2max}$ dropped significantly in the Sedentary control mice at the second time point. This is likely due to an aging effect, a phenomenon noted across all experiments in this study. Consistent with this conclusion, age-related reductions in $\dot{V}o_{2max}$ have been described in rodents, albeit at older ages (47). As expected, RER at 50% $\dot{V}o_{2max}$ was decreased in the Runner mice posttraining, consistent with training-induced increased utilization of fatty acid as fuel (Fig. 3*C*). In addition, mean state 3 mitochondrial respiration rate, determined from muscle fibers as a general measure of mitochondrial capacity, was significantly increased in Runner mice compared with Sedentary control mice (Fig. 3*D*). Lastly, a significant increase in expression of the gene encoding the oxidative MHC 2a isoform (*Myh2*) was observed in the muscle of Runner mice, consistent with an exercise-induced fiber type shift (Fig. 3*E*).

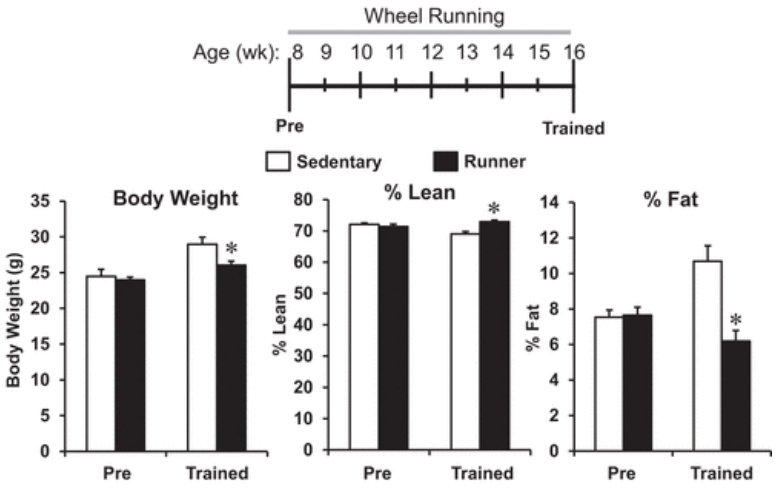

Fig. 2. Voluntary wheel running for 8 wk leads to a lean phenotype. Body weight and percent lean and fat mass were determined for mice at 8 wk (Pre) and 16 wk of age after running-wheel training (Trained). Values are means ± SE ($n \geq 6$ mice in each group). *$P < 0.05$ vs. Sedentary control (by Student's *t*-test).

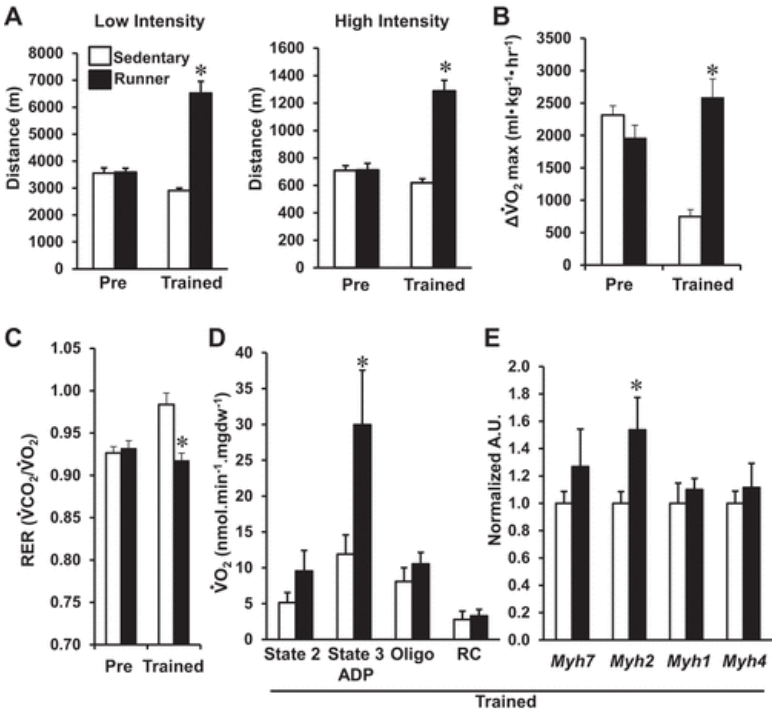

Fig. 3. Voluntary wheel running for 8 wk leads to a trained muscle phenotype. *A*: Runner mice at 8 wk (Pre) and 16 wk of age after running-wheel training (Trained) were subjected to a treadmill run-to-exhaustion protocol (a high- and low-intensity regimen). Age-matched Sedentary mice served as controls. Total running distance to exhaustion was measured as an end point. *B* and *C*: peak $\dot{V}o_2$ ($\Delta\dot{V}o_{2max}$) and respiratory exchange ratio (RER) were measured using the high-intensity protocol described in *A*. *D*: succinate-driven mitochondrial respiratory rates in saponin-permeabilized muscle strips prepared from the soleus of Sedentary and Runner mice. Rates were measured under the following conditions: basal (state 2), ADP-stimulated (state 3), and oligomycin (Oligo)-treated (state 4). Respiratory coefficient (RC) is also shown. *E*: quantitative RT-PCR assessment of expression of myosin heavy chain (MHC) genes, namely, MHC1 (*Myh7*), MHC2a (*Myh2*), MHC2x (*Myh1*), and MHC2b (*Myh4*), in gastrocnemius from Sedentary and Runner mice after 8 wk of training. Values are means ± SE ($n \geq 6$ mice in each group). Sedentary group was normalized to 1.0. Normalized arbitrary units (AU) are shown. *$P < 0.05$ vs. Sedentary control (by Student's *t*-test).

To further assess the training response and to establish muscle autonomous end points in the detraining experiments, an in situ muscle stimulation protocol was employed (27). End points were collected for soleus and plantaris muscles, with the expectation of a greater degree of training effects in the former, given that a wheel-running protocol was employed (16). After the 8-wk training regimen, generation of force was not different between Sedentary and Runner mice in either muscle (Fig. 4, *A* and *B*). In contrast, half relaxation time in the soleus, reflective of the rate of Ca^{2+} reuptake into the sarcoplasmic reticulum, was significantly less in the Runner mice, although no change was seen in the plantaris after training (Fig. 4*C*). Together, the in vivo and ex vivo measurements denote a significant endurance-training effect in the Runner mice.

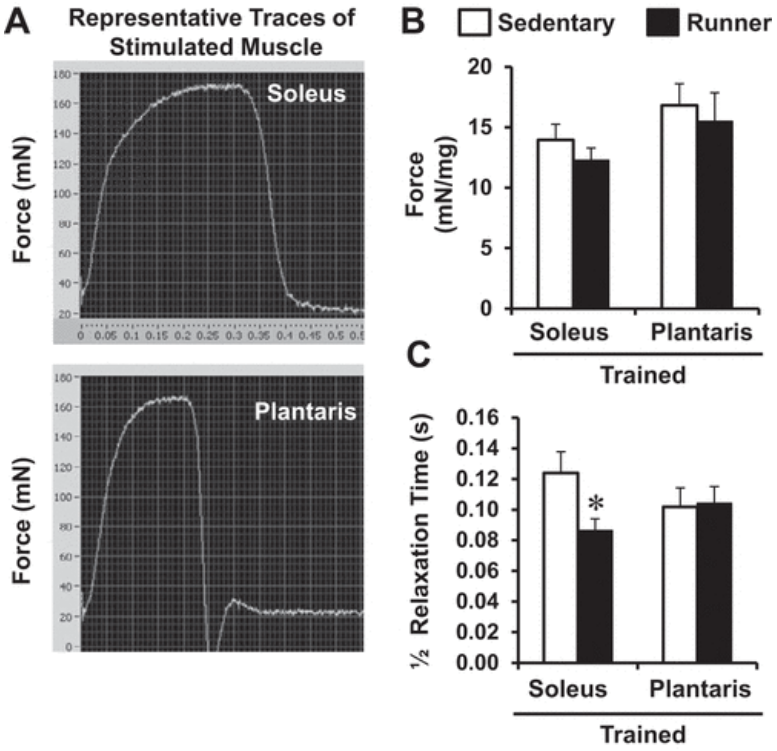

Fig. 4. Endurance training affects half relaxation time, but not peak force, in soleus muscle in an in situ preparation. *A*: representative force traces from soleus and plantaris after in situ muscle stimulation. *B*: peak force in soleus and plantaris after muscle stimulation measured using the Aurora 1300A whole mouse test system after 8 wk of training (Trained) for Runner and Sedentary (no wheel in cage) mice. *C*: half relaxation time in soleus and plantaris of mice used for traces in *A*. Values are means ± SE ($n \geq 6$ mice in each group). *$P < 0.05$ vs. Sedentary control (by Student's *t*-test).

Next, we assessed the effects of detraining over a period of 6 wk following the 8-wk training period. Detraining effects can be partial or complete. A complete loss of training was defined by loss of a significant difference in an end point compared with the Sedentary control mice at the same time point (* in Fig. 5). Partial detraining effects were defined as a significant difference between the value for the fully trained Runner mice and the value after cessation of training, yet with a training effect maintained compared with the paired Sedentary control mice (#, in absence of *, in Fig. 5). This latter comparison was possible, given that the values for the Sedentary mice across the time points were not significantly different. The increase in $\Delta\dot{V}o_{2max}$, a robust measurement of endurance training, was completely lost at 4 wk posttraining (Fig. 5*A*). Treadmill exercise performance was significantly decreased at 6 wk of detraining compared with fully trained Runner mice but was still higher than that of Sedentary control

mice at the same time point, suggesting a partial detraining response (Fig. 5*B*). Similarly, the training effect on RER was partially lost (Fig. 5*C*). Lastly, the training effect on the in situ measure of half relaxation time was completely lost by 6 wk posttraining (Fig. 5*D*).

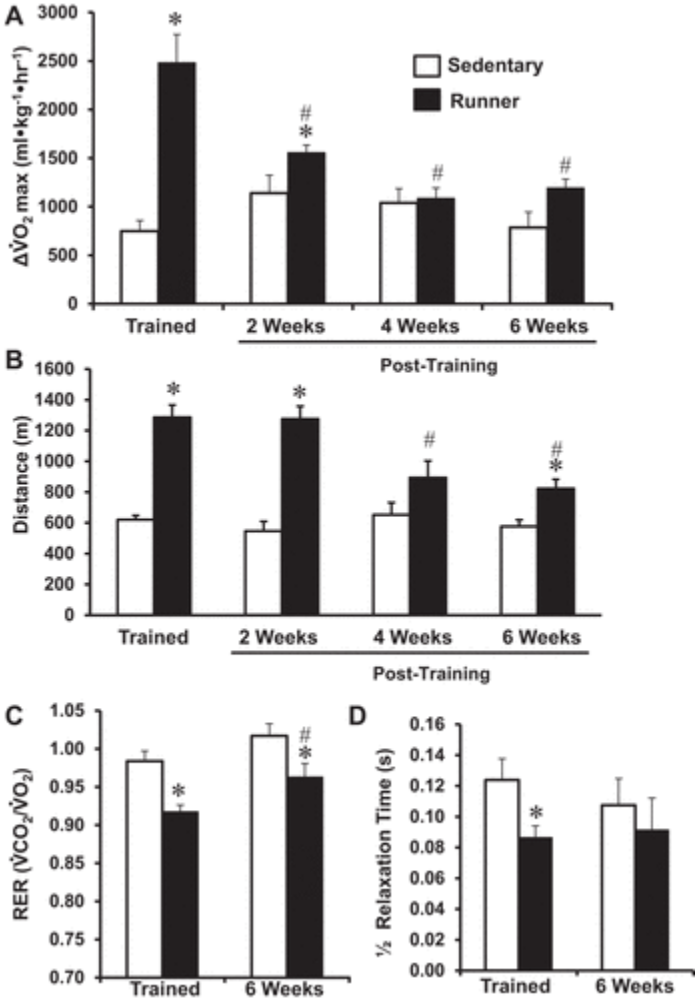

Fig. 5. Exercise fitness measurements reflect detraining effects 6 wk after cessation of endurance training. *A*: Runner mice were trained for 8 wk on a voluntary running wheel. End points were collected from age-matched Sedentary and Runner mice at 0 (Trained), 2, 4, and 6 wk following removal of the wheel. *A–C*: $\Delta\dot{V}O_{2max}$, distance to exhaustion on a treadmill, and RER in mice subjected to a high-intensity run-to-exhaustion protocol. *D*: half relaxation time in soleus. Values are means ± SE. **P* < 0.05 vs. Sedentary control at the same time point; #*P* < 0.05 vs. Runner at Trained time point (by Student's *t*-test).

Muscle-specific PGC-1β overexpression confers an "endurance fitness" phenotype in adult mice.

The transcriptional coactivators PGC-1α and -1β have been shown to mediate many of the skeletal muscle responses to exercise (3, 4, 18, 36). Therefore, we sought to determine if activation of PGC-1 signaling would have an impact on the training-detraining response. A skeletal muscle-specific, inducible, "tet-off" mouse model (51) was used to assess the effects of PGC-1-β overexpression at baseline in Sedentary mice and during the detraining period. As an initial step, we verified the induction of PGC-1β in Sedentary adult mice. PGC-1β mRNA and protein levels were induced in a skeletal muscle-specific pattern beginning 3 days after removal of doxycycline (Fig. 6, *A* and *B*). Protein

levels remained at the induced steady-state level for ≥56 days after removal of doxycycline (Fig. 6*B*). The induction of PGC-1β was specific to expression of the transgene (Fig. 6*C*). Notably, with induction of PGC-1β transgenic expression, levels of endogenous PGC-1α and -1β transcripts were significantly decreased (Fig. 6*C*), as previously shown (4). Importantly, we did not observe histological evidence of cellular or myofibrillar derangements in skeletal muscle (Fig. 6*D*). As expected, PGC-1β overexpression [TRE-PGC-1β(+)] induced known PGC-1 target genes involved in mitochondrial energy metabolism (30), including those involved in the tricarboxylic acid cycle, oxidative phosphorylation, and fatty acid β-oxidation (Fig. 7*A*). In addition, mtDNA and *Tfam* levels were increased, suggesting an increase in mitochondrial biogenesis (Fig. 7*B*). Consistent with previous studies showing that PGC-1β stimulates angiogenesis (2, 10, 44), CD31 staining was increased 4 and 8 wk after PGC-1β induction (Fig. 7*C*). Lastly, as predicted by the work of others (4), the MHC2x (*Myh1* isoform) fiber gene was selectively induced (Fig. 7*D*). MHC immunofluorescence of the glycolytic and oxidative regions of the gastrocnemius also demonstrated an increase in type IIx fibers with PGC-1β overexpression (Fig. 7*E*).

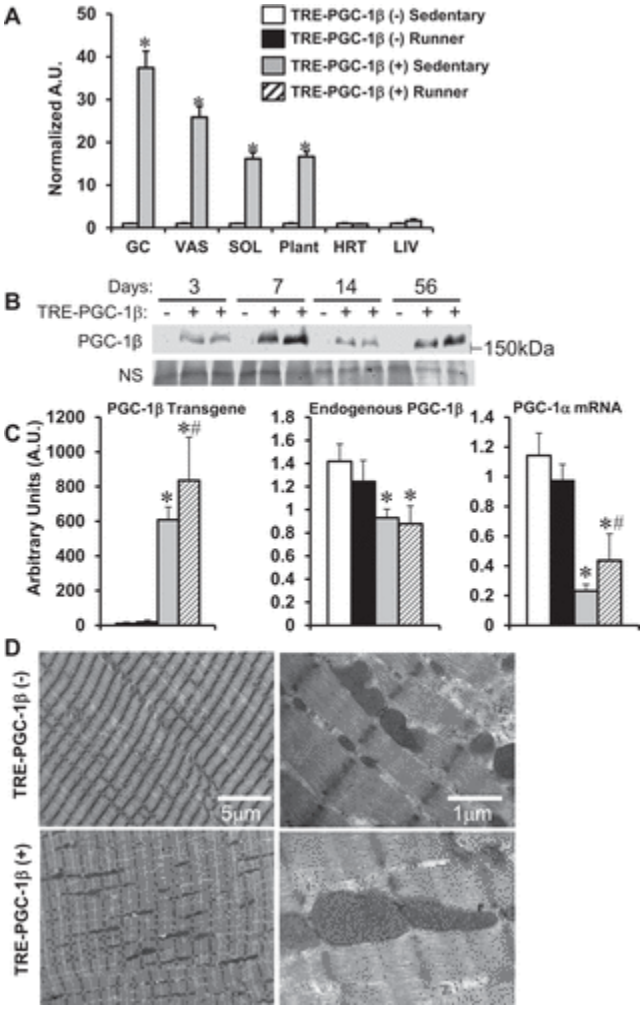

Fig. 6. PGC-1β is significantly expressed 3 days after doxycycline removal, and long-term induction of PGC-1β expression is not detrimental to the myofibrillar structure. *A*: relative PGC-1β mRNA levels (70 days after doxycycline removal) in gastrocnemius (GC), white vastus (VAS), soleus (SOL), and plantaris (Plant) of Sedentary mice. Heart (HRT) and liver (LIV) are shown as negative controls. Values are means ± SE (n = 4–6/group; quantitative RT-PCR was performed in triplicate). *P < 0.05 vs. TRE-PGC-1β(−) control. *B*: Western blot of PGC-1β protein levels in gastrocnemius at 3, 7, 14, and 56 days after removal of doxycycline. NS, nonspecific band to show control for loading. *C*: levels of the PGC-1β transgene transcript (flag-specific primer set, *left*), endogenous PGC-1β transcript (*middle*), and PGC-1α transcript (*right*) 8 wk after doxycycline

removal (all groups) and 6 wk after removal of the running wheels (Runner mice). Values are means ± SE (*n* = 6–7/group). **P* < 0.05 vs. TRE-PGC-1β(−) Sedentary; #*P* < 0.05, TRE-PGC-1β(+) Runner vs. TRE-PGC-1β(−) Runner. *D*: electron micrographs of the soleus in mice 6 wk after doxycycline removal indicate no ultrastructural derangements with PGC-1β overexpression.

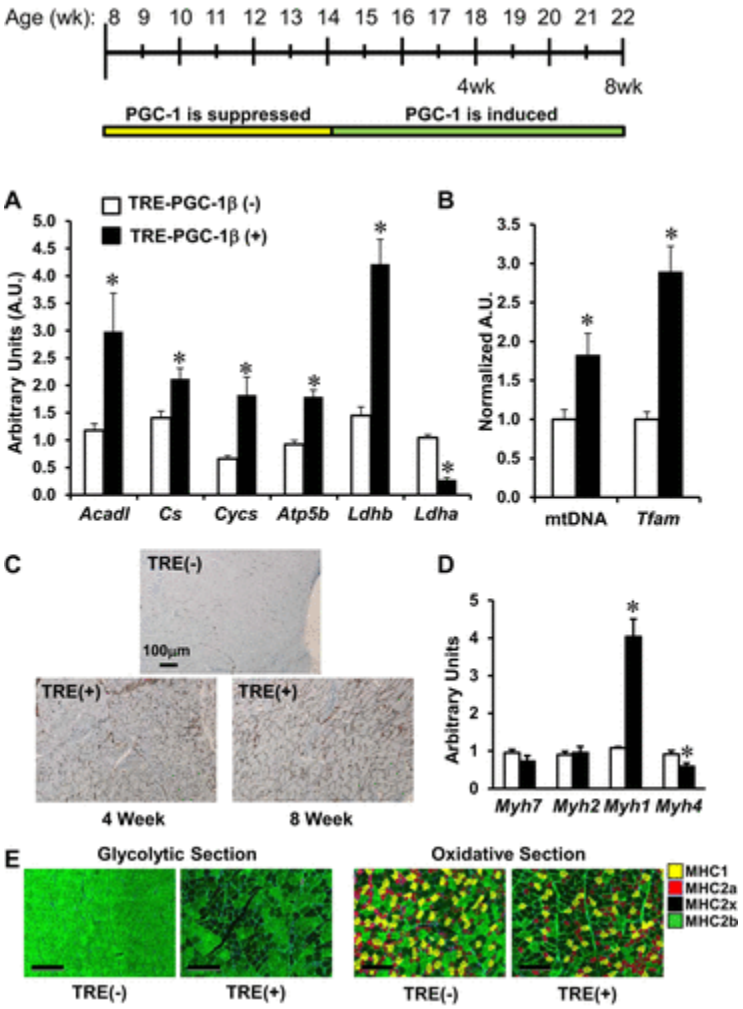

Fig. 7. Muscle-specific PGC-1β overexpression in Sedentary mice activates known training-induced gene expression markers and induces angiogenesis. *A*: mRNA levels of the mitochondrial genes citrate synthase (*Cs*), cytochrome *c* (*Cycs*), ATP synthase-β (*Atp5b*), lactate dehydrogenase A and B (*Ldha* and *Ldhb*), and long-chain acyl-CoA dehydrogenase (*Acadl*) in gastrocnemius 8 wk after doxycycline removal. Values are means ± SE (*n* = 5–8/group). *B*: mitochondrial DNA (mtDNA) levels, determined as ratio of mitochondrial- to nuclear-encoded DNA, and mitochondrial transcription factor A (*Tfam*) gene expression levels (quantitative RT-PCR) in the samples described in *A*. Values are means ± SE (*n* = 6–8/group). TRE-PGC-1β(−) was normalized to 1.0. *C*: representative images of CD31 staining of gastrocnemius muscle 4 and 8 wk postinduction (after doxycycline removal) of PGC-1β expression. Positive staining is denoted by brown color. *D*: mRNA levels encoding MHC gene isoforms MHC1 (*Myh7*), MHC2a (*Myh2*), MHC2x (*Myh1*), and MHC2b (*Myh4*) in gastrocnemius 8 wk after doxycycline removal. Values are means ± SE (*n* = 8/group). **P* < 0.05 vs. TRE-PGC-1β(−) (by Student's *t*-test). *E*: representative sections of oxidative and glycolytic regions of gastrocnemius from Sedentary TRE-PGC-1β(−) and TRE-PGC-1β(+) mice 8 wk after doxycycline removal were stained for MHC1 (yellow), MHC2a (red), and MHC2b (green). Unstained (black) fibers are MHC2x. Scale bars = 200 μm. Note increase in black (unstained) fibers in TRE-PGC-1β(+) muscle, consistent with increased proportion of MHC2x fibers.

The functional impact of PGC-1β overexpression on the trained phenotype was assessed independent of the training regimen by comparison of TRE-PGC-1β(−) Sedentary and TRE-PGC-1β(+) Sedentary mice. Induction of PGC-1β significantly increased $\Delta\dot{V}O_{2max}$ (Fig. 8*A*) and decreased RER (Fig. 8*B*) by 6 wk after doxycyline removal. In addition, performance on the run-to-exhaustion test was increased by 2 wk (Fig. 8*C*) and 4 wk (data not shown) after doxycycline removal, but this effect was no longer present at 6 wk (Fig. 8*C*). The reason for this latter observation is not clear but could relate to adaptation to the treadmill-running protocol after serial testing due to learned behavior related to tolerating the shock stimulus that results in cessation of the protocol. Together, these results confirmed that the inducible transgenic system was operational and that overexpression of PGC-1β was sufficient to induce a robust endurance muscle phenotype, independent of exercise.

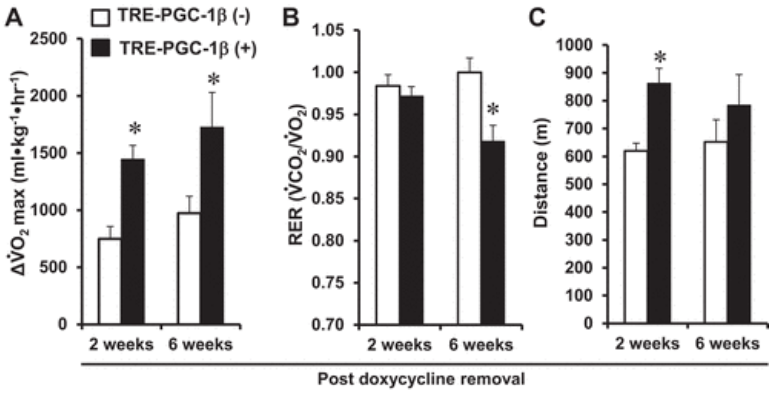

Fig. 8. PGC-1β overexpression in muscle mimics effects of training in Sedentary mice. *A–C*: $\Delta\dot{V}O_{2max}$, RER, and distance to exhaustion on a treadmill during a high-intensity run-to-exhaustion protocol for TRE-PGC-1β(−) and TRE-PGC-1β(+) mice. End points were collected 2 and 6 wk following doxycycline removal. Values are means ± SE. **P* < 0.05 vs. TRE-PGC-1β(−) controls at the same time point (by Student's *t*-test).

Effects of muscle PGC-1β on detraining.

To assess the effects of induction of PGC-1β on the detraining response, TRE-PGC-1β(−) Runner and TRE-PGC-1β(+) Runner mice were compared 6 wk after removal of the running wheels (8 wk after doxycycline removal and induction of PGC-1β transgene expression; Fig. 1). $\Delta\dot{V}O_{2max}$ was significantly higher in the TRE-PGC-1β(+) Runner than the TRE-PGC-1β(−) Runner mice following 6 wk of detraining but was significantly lower than in the fully trained mice, indicative of partial prevention of this detraining response (Fig. 9*A*). In addition, RER was lower (*P* = 0.06) in the TRE-PGC-1β(+) Runner than TRE-PGC-1β(−) Runner mice at the end of the detraining period (Fig. 9*B*). However, there was no difference in running performance based on the treadmill "distance-to-exhaustion" parameter at any time between the two groups (Fig. 9*C*). Similarly, PGC-1β overexpression did not impact the training effect on in situ muscle stimulation studies and, generally, did not demonstrate an effect of PGC-1β on detraining (Fig. 9*C*).

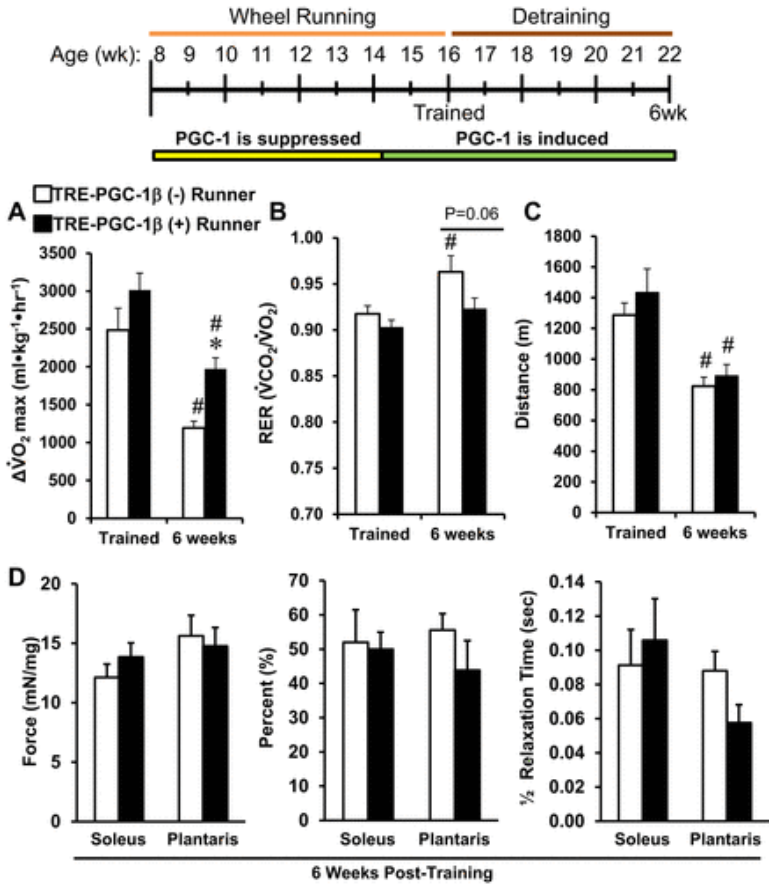

Fig. 9. Muscle-specific PGC-1β overexpression reduces detraining effect on $\dot{V}O_{2max}$. Mice were run on a treadmill according to a run-to-exhaustion protocol (a high-intensity regimen) 6 wk after cessation of training on a voluntary running wheel (Runner mice) and 8 wk after removal of doxycycline to induce PGC-1β expression in TRE-PGC-1β(+) mice compared with TRE-PGC-1β(−) mice. *A–C*: $\Delta\dot{V}O_{2max}$, RER, and total distance to exhaustion. Values are means ± SE. *D*: peak force, percent reduction in force after 20 min of electrical stimulation (measure of fatigue), and half relaxation time in soleus and plantaris in a separate cohort of mice at 6 wk posttraining after muscle stimulation using the Aurora 1300A Whole Mouse Test System. Values are means ± SE (n = 5–8/group). *P < 0.05 vs. TRE-PGC-1β(−) controls at the same time point; #P < 0.05 vs. Trained time point of the same group (by Student's t-test).

The results of the detraining studies indicated that only a subset of end points was impacted by induction of PGC-1β expression in muscle. Specifically, training-induced changes in $\dot{V}O_{2max}$ and RER end points were observed at 6 wk posttraining (Fig. 9, *A* and *B*), whereas running performance and in situ muscle fatigability were unaffected (Fig. 9, *C* and *D*). These results suggest that the PGC-1β-induced endurance phenotype is unable to fully defend against detraining. We assessed other components of the training response to confirm that known PGC-1β target responses were being activated in mouse muscle following cessation of training. First, we found an increase in the expression of downstream PGC-1 effectors, including *Esrra* and *Esrrb* (Fig. 10*A*), along with an induction of corresponding downstream targets, including *Ldhb*, a known marker of exercise training, mtDNA, and *Tfam* expression levels (Fig. 10*B*). In addition, levels of CD31/*Pecam*-1 and MHC2x transcripts were induced (Figs. 10, *C* and *D*) in muscle of TRE-PGC-1β(+) compared with TRE-PGC-1β(−) Runner mice. These results indicate that the known target actions of PGC-1 in muscle were also observed during the detraining period but that this is insufficient to prevent all functional changes during detraining.

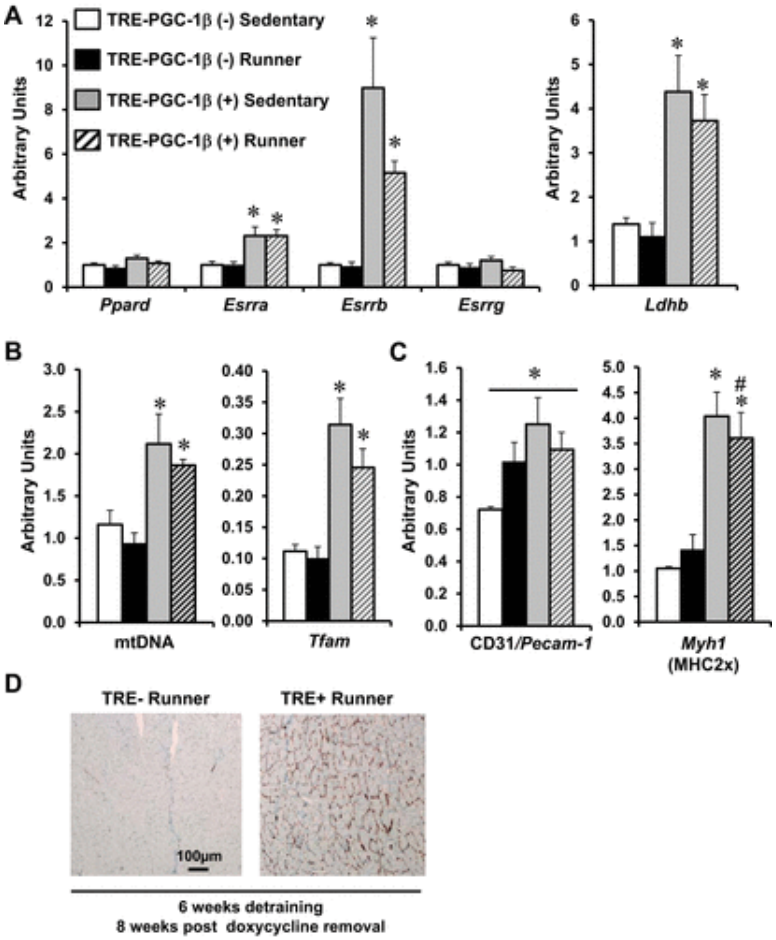

Fig. 10. Overexpression of PGC-1β activates known downstream targets in muscle during the detraining period. *A–C*: relative transcript expression levels for nuclear transcription factors/genes [peroxisome proliferator-activated receptor-δ (*Ppard*), estrogen-related receptor (EsRR)-α, -β, and -γ (*Esrra, Esrrb*, and *Esrrg*), lactate dehydrogenase A (*Ldha*), mitochondrial transcription factor A (*Tfam*), platelet and endothelial cell adhesion molecule 1 (*Pecam-1*), and MHC2x (*Myh1*)] 8 wk after removal of doxycycline (6 wk of detraining). mtDNA is a measure of mitochondrial/genomic DNA. Values are means ± SE ($n \geq 6$ mice in each group). *$P < 0.05$ vs. TRE-PGC-1β(−) Sedentary controls; #$P < 0.05$ vs. TRE-PGC-1β(−) Runner mice (by Student's *t*-test). *D*: representative images of CD31 staining of gastrocnemius muscle from TRE-PGC-1β(−) Runner and TRE-PGC-1β(+) Runner mice 6 wk posttraining.

DISCUSSION

The muscle endurance-detraining response is well recognized but poorly understood. Delineation of the mechanisms involved in muscle detraining could lead to the discovery of new therapeutic strategies to reverse this process in a variety of injury and disease states. The wheel-running-based protocol described here allowed us to assess training and detraining responses in mice. Our collective results led to the following conclusions. *1*) Muscle-specific induction of PGC-1β expression, using a conditional transgenic system, is sufficient to phenocopy the effects of endurance exercise training in Sedentary (nontrained) mice. *2*) Induction of PGC-1β in combination with exercise training does not enhance the endurance phenotype beyond exercise alone. *3*) Muscle-specific induction of PGC-1β prevents some, but not all, components of the detraining response, suggesting that mechanisms independent of the exercised-induced muscle endurance fitness circuitry, as mimicked by activation of

PGC-1β signaling, contribute to detraining. Accordingly, the physiological reprogramming that contributes to the detraining response likely involves muscle autonomous and nonautonomous inputs.

We found that muscle-specific overexpression of the transcriptional coregulator PGC-1β resulted in an endurance-trained phenotype in sedentary mice. This observation is consistent with the results of previous studies demonstrating that muscle-specific PGC-1β transgenes are capable of enhanced performance on low-intensity treadmill regimens (4) and exhibit increased muscle capillary density (44). Our results demonstrate that forced expression of PGC-1β results in a significant endurance-training effect within 2 wk (Fig. 8). An array of end points, including treadmill performance, $\dot{V}o_{2max}$ and RER, gene markers of mitochondrial function and fiber type, and vascular density, support this conclusion. The majority of the endurance end points identified in wild-type mice trained on running wheels, including gene markers of mitochondrial biogenesis, enhanced treadmill running time, increased $\dot{V}o_{2max}$, reduced RER, and angiogenesis, were also triggered by PGC-1β overexpression in sedentary mice.

A key difference in the endurance phenotype in wheel-running vs. TRE-PGC-1β(+) Sedentary mice was the effect on fiber type proportion, as determined by gene markers. As described by others, we observed an increase in *Myh2* (MHC2a gene) expression in TRE-PGC-1β(−) Runner gastrocnemius muscle. In contrast, TRE-PGC-1β(+) Sedentary mice exhibited a selective increase in *Myh1* (MHC2x gene) expression and immunostaining without a change in *Myh2* expression. Selective induction of *Myh1* expression has been described in muscle of PGC-1β transgenes (4). The functional relevance of type IIx fibers in mice, including contribution to the endurance phenotype in TRE-PGC-1β(+) mice, is unknown. Previous studies have shown that the related transcriptional coactivator PGC-1α is also capable of inducing an endurance-training phenotype in muscle-specific transgenic mice (35, 49). However, PGC-1α overexpression in muscle induces a classic oxidative fiber type switch (35), in contrast to the *Myh1* selectivity described here with PGC-1β. Together, these observations suggest that PGC-1α and -1β regulate both overlapping and distinct target genes in muscle.

Given that muscle PGC-1β overexpression was sufficient to drive an endurance phenotype, we assessed the impact of this intervention during detraining. It is interesting that only a subset of detraining responses was prevented by PGC-1β overexpression [TRE-PGC-1β(+) Runner vs. TRE-PGC-1β(−) Runner mice]. Importantly, the loss of the training-induced increase in $\dot{V}o_{2max}$ in the TRE-PGC-1β(−) Runner mice during detraining was significantly less in the TRE-PGC-1β(+) Runner mice. The main factors that influence $\dot{V}o_{2max}$, a key determinant of endurance fitness, include O_2 supply (O_2 transport to the muscle) and demand (including capacity for mitochondrial oxidative phosphorylation). Consistent with the effects on $\dot{V}o_{2max}$, we found that vascular density and markers of mitochondrial biogenesis were maintained during the detraining period in the TRE-PGC-1β(+) Runner mice. In contrast to the $\dot{V}o_{2max}$ results, functional detraining responses, including running time and contractile function (in situ muscle stimulation), were not different between the detrained TRE-PGC-1β(+) and TRE-PGC-1β(−) Runner mice. These results, together with the endurance phenotype of PGC-1β overexpression in the Sedentary mice, suggest that the detraining response involves more than simply deactivation of the muscle training response.

The interesting discrepancy between the PGC-1β-driven endurance phenotype in the Sedentary transgenic animals and the mixed results during the detraining period could theoretically reflect a

time-related diminution of the impact of PGC-1β. However, this seems highly unlikely, given that several fitness parameters noted to be maintained during the detraining period in the exercised animals were also maintained in the Sedentary TRE-PGC-1β(+) mice at the same time points. Specifically, $\Delta\dot{V}o_{2max}$ and RER remained significantly different in Sedentary PGC-1β-overexpressing animals vs. nontransgenic mice at late time points during the detraining period. In contrast, other parameters, such as run-to-exhaustion and contractility measurements, were not maintained during the late time periods in the exercised-detrained transgenic group. In the case of the run-to-exhaustion parameter, it is possible that a learned behavior changed the accuracy of this end point and precludes its use over time. Together, however, we do not believe that time-related changes in the efficacy of the PGC-1β transgene explain the interesting observation that only a subset of end points was maintained during detraining. Rather, only a subset of endurance-training responses was maintained during detraining, despite PGC-1β overexpression.

The interesting observation that PGC-1β overexpression cannot maintain all endurance parameters during detraining suggests that some detraining effects are external to muscle and, therefore, are not affected by our transgenic strategy. For example, reductions in blood volume, red blood cell mass, and cardiac output are muscle nonautonomous factors known to influence endurance performance (39). In addition, effects related to neural circuitry or hepatic glucose production converging on muscle could be at play. Alternatively, or in addition, the selective maintenance in *Myh1*-rich fibers, without corresponding induction of *Myh2*-rich fibers, as typically seen in an endurance response, may be insufficient to prevent the performance abnormalities that occur with detraining. Future studies, with interventions that are known to mimic the increase in oxidative fibers, along with the other responses, will be important in this regard.

The protocol employed here results in a robust endurance-trained phenotype followed by detraining in FVB mice. We collected a panel of end points that measure molecular, cellular, and functional responses to endurance training and detraining. This protocol should prove useful for studies aimed at assessing the impact of genetic, pharmacological, physiological, or dietary interventions on the endurance-training and -detraining phenotypes. Importantly, the use of an extensive panel of end points allows identification of effects on individual components of the muscle-detraining responses, as observed in this study with the PGC-1β intervention. We propose that successful prevention of the detraining response may require a combination of therapeutic approaches to prevent or treat the pleiotropic responses of detraining. Protocols such as the approach described here are necessary to assess such combinatorial approaches.

In summary, our results suggest that the process of endurance detraining involves mechanisms beyond the reversal of muscle autonomous mechanisms involved in endurance fitness. However, the observation that PGC-1β is capable of impacting a subset of the muscle-detraining responses suggests that therapeutic approaches, possibly in combination with targeting PGC-1β, could be effective in reducing or preventing the untoward effects of detraining.

GRANTS

This work was supported by US Department of Defense Grant W81XWH-11-1-0764 (D. P. Kelly) and National Institute of Diabetes and Digestive and Kidney Diseases Grant R01 DK-045416 (D. P. Kelly). P. M. Coen is supported by National Institute on Aging Career Development Award K01 AG-044437.

DISCLOSURES

D. P. Kelly is a scientific consultant for Pfizer, Inc., and received research support from Takeda Pharmaceutical Co. R. B. Vega received research support from Pfizer, Inc. P. M. Coen is a scientific consultant for Mitobridge, Inc.

AUTHOR CONTRIBUTIONS

S.L., L.R., J.R., and J.A. performed the experiments; S.L., T.C.L., L.R., J.R., J.A., R.H.F., and R.B.V. analyzed the data; S.L., T.C.L., and L.R. prepared the figures; S.L., T.C.L., L.R., J.R., J.A., P.M.C., R.H.F., R.B.V., and D.P.K. edited and revised the manuscript; S.L., T.C.L., L.R., J.R., J.A., P.M.C., R.H.F., R.B.V., and D.P.K. approved the final version of the manuscript; T.C.L. and D.P.K. conceived and designed the research; T.C.L., J.A., P.M.C., R.H.F., R.B.V., and D.P.K. interpreted the results of the experiments; T.C.L. and D.P.K. drafted the manuscript.

ACKNOWLEDGMENTS

We thank Lorenzo Thomas for assistance with manuscript preparation; Jeanne Brooks and Ling Lai for excellent technical assistance; Orlando Rodriguez and Caron Stonebrook for assistance with the animal studies; the Sanford Burnham Prebys (SBP) Cardiometabolic Phenotyping Core for the $\Delta\dot{V}o_{2max}$ and RER studies; and the SBP Histology Core for CD31 and MHC staining and electron microscopy.

AUTHOR NOTES

- [*]S. Lee and T. C. Leone contributed equally to this work.
- Address for reprint requests and other correspondence: D. P. Kelly, Sanford Burnham Prebys Medical Discovery Institute, 6400 Sanger Rd., Orlando, FL 32827 (e-mail: dkelly@sbpdiscovery.org).

REFERENCES

1. Andersen JL, Schjerling P, Andersen LL, Dela F. Resistance training and insulin action in humans: effects of de-training. *J Physiol* 551:1049–1058, 2003. doi:10.1113/jphysiol.2003.043554.
2. Arany Z, Foo SY, Ma Y, Ruas JL, Bommi-Reddy A, Girnun G, Cooper M, Laznik D, Chinsomboon J, Rangwala SM, Baek KH, Rosenzweig A, Spiegelman BM. HIF-independent regulation of VEGF and angiogenesis by the transcriptional coactivator PGC-1α. *Nature* 451: 1008–1012, 2008. doi:10.1038/nature06613.
3. Arany Z, He H, Lin J, Hoyer K, Handschin C, Toka O, Ahmad F, Matsui T, Chin S, Wu PH, Rybkin II, Shelton JM, Manieri M, Cinti S, Schoen FJ, Bassel-Duby R, Rosenzweig A, Ingwall JS, Spiegelman BM. Transcriptional coactivator PGC-1α controls the energy state and contractile function of cardiac muscle. *Cell Metab* 1: 259–271, 2005. doi:10.1016/j.cmet.2005.03.002.
4. Arany Z, Lebrasseur N, Morris C, Smith E, Yang W, Ma Y, Chin S, Spiegelman BM. The transcriptional coactivator PGC-1β drives the formation of oxidative type IIX fibers in skeletal muscle. *Cell Metab* 5: 35–46, 2007. doi:10.1016/j.cmet.2006.12.003.

5. Arciero PJ, Smith DL, Calles-Escandon J. Effects of short-term inactivity on glucose tolerance, energy expenditure, and blood flow in trained subjects. *J Appl Physiol (1985)* 84: 1365–1373, 1998.
6. Ayala JE, Bracy DP, James FD, Julien BM, Wasserman DH, Drucker DJ. The glucagon-like peptide-1 receptor regulates endogenous glucose production and muscle glucose uptake independent of its incretin action. *Endocrinology* 150: 1155–1164, 2009. doi:10.1210/en.2008-0945.
7. Baar K, Wende AR, Jones TE, Marison M, Nolte LA, Chen M, Kelly DP, Holloszy JO. Adaptations of skeletal muscle to exercise: rapid increase in the transcriptional coactivator PGC-1. *FASEB J* 16: 1879– 1886, 2002. doi:10.1096/fj.02-0367com.
8. Bell KE, von Allmen MT, Devries MC, Phillips SM. Muscle disuse as a pivotal problem in sarcopenia-related muscle loss and dysfunction. *J Frailty Aging* 5: 33–41, 2016.
9. Calvo JA, Daniels TG, Wang X, Paul A, Lin J, Spiegelman BM, Stevenson SC, Rangwala SM. Muscle-specific expression of PPARγ coactivator-1α improves exercise performance and increases peak oxygen uptake. *J Appl Physiol (1985)* 104: 1304–1312, 2008. doi:10.1152/japplphysiol.01231.2007.
10. Chinsomboon J, Ruas J, Gupta RK, Thom R, Shoag J, Rowe GC, Sawada N, Raghuram S, Arany Z. The transcriptional coactivator PGC-1α mediates exercise-induced angiogenesis in skeletal muscle. *Proc Natl Acad Sci USA* 106: 21401–21406, 2009. doi:10.1073/pnas.0909131106.
11. Coyle EF, Martin WH 3rd, Sinacore DR, Joyner MJ, Hagberg JM, Holloszy JO. Time course of loss of adaptations after stopping prolonged intense endurance training. *J Appl Physiol Respir Environ Exerc Physiol* 57: 1857–1864, 1984.
12. Dai B, Sorensen CJ, Derrick TR, Gillette JC. The effects of postseason break on knee biomechanics and lower extremity EMG in a stop-jump task: implications for ACL injury. *J Appl Biomech* 28: 708–717, 2012. doi:10.1123/jab.28.6.708.
13. Daugaard JR, Nielsen JN, Kristiansen S, Andersen JL, Hargreaves M, Richter EA. Fiber type-specific expression of GLUT4 in human skeletal muscle: influence of exercise training. *Diabetes* 49: 1092–1095, 2000. doi:10.2337/diabetes.49.7.1092.
14. Eisele PS, Furrer R, Beer M, Handschin C. The PGC-1 coactivators promote an anti-inflammatory environment in skeletal muscle in vivo. *Biochem Biophys Res Commun* 464: 692–697, 2015. doi:10.1016/j.bbrc.2015.06.166.
15. Finck BN, Kelly DP. PGC-1 coactivators: inducible regulators of energy metabolism in health and disease. *J Clin Invest* 116: 615–622, 2006. doi:10.1172/JCI27794.
16. Fitts RH, Holloszy JO. Contractile properties of rat soleus muscle: effects of training and fatigue. *Am J Physiol Cell Physiol* 233: C86–C91, 1977. 17. Gali Ramamoorthy T, Laverny G, Schlagowski AI, Zoll J, Messaddeq N, Bornert JM, Panza S, Ferry A, Geny B, Metzger D. The transcriptional coregulator PGC-1β controls mitochondrial function and antioxidant defence in skeletal muscles. *Nat Commun* 6: 10210, 2015. doi: 10.1038/ncomms10210.
18. Geng T, Li P, Okutsu M, Yin X, Kwek J, Zhang M, Yan Z. PGC-1α plays a functional role in exercise-induced mitochondrial biogenesis and angiogenesis but not fiber-type transformation in mouse skeletal muscle. *Am J Physiol Cell Physiol* 298: C572–C579, 2010. doi:10.1152/ajpcell.00481.2009.
19. Ghersa P, Gobert RP, Sattonnet-Roche P, Richards CA, Merlo Pich E, Hooft van Huijsduijnen R. Highly controlled gene expression using combinations of a tissue-specific promoter, recombinant adenovirus and a tetracycline-regulatable transcription factor. *Gene Ther* 5: 1213–1220, 1998. doi:10.1038/sj.gt.3300713.
20. Goss DL, Christopher GE, Faulk RT, Moore J. Functional training program bridges rehabilitation and return to duty. *J Spec Oper Med* 9: 29–48, 2009.
21. Goto M, Terada S, Kato M, Katoh M, Yokozeki T, Tabata I, Shimokawa T. cDNA Cloning and mRNA analysis of PGC-1 in epitrochlearis muscle in swimming-exercised rats. *Biochem Biophys Res Commun* 274: 350–354, 2000. doi:10.1006/bbrc.2000.3134.
22. Handschin C, Chin S, Li P, Liu F, Maratos-Flier E, Lebrasseur NK, Yan Z, Spiegelman BM. Skeletal muscle fiber-type switching, exercise intolerance, and myopathy in PGC-1α muscle-specific knock-out animals. *J Biol Chem* 282: 30014–30021, 2007. doi:10.1074/jbc.M704817200.

23. Hawley JA, Holloszy JO. Exercise: it's the real thing! *Nutr Rev* 67: 172–178, 2009. doi:10.1111/j.1753-4887.2009.00185.x.
24. Henriksen EJ, Bourey RE, Rodnick KJ, Koranyi L, Permutt MA, Holloszy JO. Glucose transporter protein content and glucose transport capacity in rat skeletal muscles. *Am J Physiol Endocrinol Metab* 259: E593–E598, 1990.
25. Holloszy JO. Regulation by exercise of skeletal muscle content of mitochondria and GLUT4. *J Physiol Pharmacol* 59, *Suppl* 7: 5–18, 2008.
26. Houston ME, Bentzen H, Larsen H. Interrelationships between skeletal muscle adaptations and performance as studied by detraining and retraining. *Acta Physiol Scand* 105: 163–170, 1979. doi:10.1111/j.1748-1716.1979.tb06328.x.
27. Hurst JE, Fitts RH. Hindlimb unloading-induced muscle atrophy and loss of function: protective effect of isometric exercise. *J Appl Physiol (1985)* 95: 1405–1417, 2003. doi:10.1152/japplphysiol.00516.2002.
28. Kaufman KR, Brodine S, Shaffer R. Military training-related injuries: surveillance, research, and prevention. *Am J Prev Med* 18, *Suppl*: 54–63, 2000. doi:10.1016/S0749-3797(00)00114-8.
29. Klausen K, Andersen LB, Pelle I. Adaptive changes in work capacity, skeletal muscle capillarization and enzyme levels during training and detraining. *Acta Physiol Scand* 113: 9–16, 1981. doi:10.1111/j.1748-1716.1981.tb06854.x.
30. Lai L, Leone TC, Zechner C, Schaeffer PJ, Kelly SM, Flanagan DP, Medeiros DM, Kovacs A, Kelly DP. Transcriptional coactivators PGC-1α and PGC-lβ control overlapping programs required for perinatal maturation of the heart. *Genes Dev* 22: 1948–1961, 2008. doi:10.1101/gad.1661708.
31. Lehman JJ, Barger PM, Kovacs A, Saffitz JE, Medeiros DM, Kelly DP. Peroxisome proliferator-activated receptor-γ coactivator-1 promotes cardiac mitochondrial biogenesis. *J Clin Invest* 106: 847–856, 2000. doi:10.1172/JCI10268.
32. Lelliott CJ, Medina-Gomez G, Petrovic N, Kis A, Feldmann HM, Bjursell M, Parker N, Curtis K, Campbell M, Hu P, Zhang D, Litwin SE, Zaha VG, Fountain KT, Boudina S, Jimenez-Linan M, Blount M, Lopez M, Meirhaeghe A, Bohlooly-Y M, Storlien L, Strömstedt M, Snaith M, Oresic M, Abel ED, Cannon B, Vidal-Puig A. Ablation of PGC-1β results in defective mitochondrial activity, thermogenesis, hepatic function, and cardiac performance. *PLoS Biol* 4: e369, 2006. doi:10.1371/journal.pbio.0040369.
33. Leone TC, Lehman JJ, Finck BN, Schaeffer PJ, Wende AR, Boudina S, Courtois M, Wozniak DF, Sambandam N, Bernal-Mizrachi C, Chen Z, Holloszy JO, Medeiros DM, Schmidt RE, Saffitz JE, Abel ED, Semenkovich CF, Kelly DP. PGC-1α deficiency causes multi-system energy metabolic derangements: muscle dysfunction, abnormal weight control and hepatic steatosis. *PLoS Biol* 3: e101, 2005. doi:10.1371/journal.pbio.0030101.
34. Lillioja S, Young AA, Culter CL, Ivy JL, Abbott WG, Zawadzki JK, Yki-Järvinen H, Christin L, Secomb TW, Bogardus C. Skeletal muscle capillary density and fiber type are possible determinants of in vivo insulin resistance in man. *J Clin Invest* 80: 415–424, 1987. doi:10.1172/JCI113088.
35. Lin J, Wu H, Tarr PT, Zhang CY, Wu Z, Boss O, Michael LF, Puigserver P, Isotani E, Olson EN, Lowell BB, Bassel-Duby R, Spiegelman BM. Transcriptional co-activator PGC-1α drives the formation of slow-twitch muscle fibres. *Nature* 418: 797–801, 2002. doi:10.1038/nature00904.
36. Lira VA, Benton CR, Yan Z, Bonen A. PGC-1α regulation by exercise training and its influences on muscle function and insulin sensitivity. *Am J Physiol Endocrinol Metab* 299: E145–E161, 2010. doi:10.1152/ajpendo.00755.2009.
37. Malek MH, Olfert IM, Esposito F. Detraining losses of skeletal muscle capillarization are associated with vascular endothelial growth factor protein expression in rats. *Exp Physiol* 95: 359–368, 2010. doi:10.1113/expphysiol.2009.050369.
38. Martin OJ, Lai L, Soundarapandian MM, Leone TC, Zorzano A, Keller MP, Attie AD, Muoio DM, Kelly DP. A role for peroxisome proliferator-activated receptor γ coactivator-1 in the control of mitochondrial dynamics during postnatal cardiac growth. *Circ Res* 114: 626–636, 2014. doi:10.1161/CIRCRESAHA.114.302562.

39. Mujika I, Padilla S. Detraining: loss of training-induced physiological and performance adaptations. II. Long term insufficient training stimulus. *Sports Med* 30: 145–154, 2000. doi:10.2165/00007256-200030030-00001.
40. Mujika I, Padilla S. Muscular characteristics of detraining in humans. *Med Sci Sports Exerc* 33: 1297–1303, 2001. doi:10.1097/00005768-200108000-00009.
41. Narkar VA, Downes M, Yu RT, Embler E, Wang YX, Banayo E, Mihaylova MM, Nelson MC, Zou Y, Juguilon H, Kang H, Shaw RJ, Evans RM. AMPK and PPARδ agonists are exercise mimetics. *Cell* 134: 405–415, 2008. doi:10.1016/j.cell.2008.06.051.
42. Neufer PD. The effect of detraining and reduced training on the physiological adaptations to aerobic exercise training. *Sports Med* 8: 302–320, 1989. doi:10.2165/00007256-198908050-00004.
43. Pilegaard H, Saltin B, Neufer PD. Exercise induces transient transcriptional activation of the PGC-1α gene in human skeletal muscle. *J Physiol* 546: 851–858, 2003. doi:10.1113/jphysiol.2002.034850.
44. Rowe GC, Jang C, Patten IS, Arany Z. PGC-1β regulates angiogenesis in skeletal muscle. *Am J Physiol Endocrinol Metab* 301: E155–E163, 2011. doi:10.1152/ajpendo.00681.2010.
45. Saks VA, Veksler VI, Kuznetsov AV, Kay L, Sikk P, Tiivel T, Tranqui L, Olivares J, Winkler K, Wiedemann F, Kunz WS. Permeabilized cell and skinned fiber techniques in studies of mitochondrial function in vivo. *Mol Cell Biochem* 184: 81–100, 1998. doi:10.1023/A:1006834912257.
46. Saltin B, Henriksson J, Nygaard E, Andersen P, Jansson E. Fiber types and metabolic potentials of skeletal muscles in sedentary man and endurance runners. *Ann NY Acad Sci* 301: 3–29, 1977. doi:10.1111/j.1749-6632.1977.tb38182.x.
47. Schefer V, Talan MI. Oxygen consumption in adult and AGED C57BL/6J mice during acute treadmill exercise of different intensity. *Exp Gerontol* 31: 387–392, 1996. doi:10.1016/0531-5565(95)02032-2.
48. Song XM, Ryder JW, Kawano Y, Chibalin AV, Krook A, Zierath JR. Muscle fiber type specificity in insulin signal transduction. *Am J Physiol Regul Integr Comp Physiol* 277: R1690–R1696, 1999.
49. Tadaishi M, Miura S, Kai Y, Kano Y, Oishi Y, Ezaki O. Skeletal muscle-specific expression of PGC-1α-b, an exercise-responsive isoform, increases exercise capacity and peak oxygen uptake. *PLoS One* 6: e28290, 2011. doi:10.1371/journal.pone.0028290.
50. Waters RE, Rotevatn S, Li P, Annex BH, Yan Z. Voluntary running induces fiber type-specific angiogenesis in mouse skeletal muscle. *Am J Physiol Cell Physiol* 287: C1342–C1348, 2004. doi:10.1152/ajpcell.00247.2004.
51. Wende AR, Schaeffer PJ, Parker GJ, Zechner C, Han DH, Chen MM, Hancock CR, Lehman JJ, Huss JM, McClain DA, Holloszy JO, Kelly DP. A role for the transcriptional coactivator PGC-1α in muscle refueling. *J Biol Chem* 282: 36642–36651, 2007. doi:10.1074/jbc.M707006200.
52. Wu Z, Puigserver P, Andersson U, Zhang C, Adelmant G, Mootha V, Troy A, Cinti S, Lowell B, Scarpulla RC, Spiegelman BM. Mechanisms controlling mitochondrial biogenesis and respiration through the thermogenic coactivator PGC-1. *Cell* 98: 115–124, 1999. doi:10.1016/S0092-8674(00)80611-X.
53. Zechner C, Lai L, Zechner JF, Geng T, Yan Z, Rumsey JW, Collia D, Chen Z, Wozniak DF, Leone TC, Kelly DP. Total skeletal muscle PGC-1 deficiency uncouples mitochondrial derangements from fiber type determination and insulin sensitivity. *Cell Metab* 12: 633–642, 2010. doi:10.1016/j.cmet.2010.11.008.
54. Zierath JR, Hawley JA. Skeletal muscle fiber type: influence on contractile and metabolic properties. *PLoS Biol* 2: e348, 2004. doi:10.1371/journal.pbio.0020348.